J. Tek. Bhn. Nukl.
Vol. 3 No. 2 Juni 2007: 49–108
ISSN 1907–2635
82/Akred-LIPI/P2MBI/5/2007

THE X-RAY DIFFRACTION ANALYSES ON THE MECHANICAL ALLOYING OF THE Mg_2Ni FORMATION

Hadi Suwarno*, Andon Insani**, Wisnu Ari Adi**
* Centre for Nuclear Fuel Technology – BATAN
** Centre for Nuclear Industry Materials – BATAN
Kawasan PUSPIPTEK, Tangerang 15314

ABSTRACT

THE X-RAY DIFFRACTION ANALYSES ON THE MECHANICAL ALLOYING OF THE Mg_2Ni FORMATION. The synthesis and characterization of Mg_2Ni compound by using mechanical alloying technique have been performed. The material is milled under the varied milling time of 20, 25, 30, 35 and 40 hours. The result of measurements by using X-ray diffractometer showed that the refinement results on X-ray diffraction pattern appear to be very good fitting between calculation and observation. It is shown that the specimens consist of three phases, namely Mg_2Ni, MgO and $MgNi_2$. For milling time between 20 hours to 25 hours, the mass fraction of the Mg_2Ni phase increases from 42.19% to 51.03%. Continuous milling of the specimen up to 40 hours will reduce the Mg_2Ni mass fraction to 11.86%, probably due to the presence of oxygen, and consequently will increase the mass fraction of $MgNi_2$ compound. It is concluded that the milling time will influence the formation of Mg_2Ni phase. At this research, 25 hours milling time is the best time to obtain the highest formation of Mg_2Ni compound. Microstructure analyses of the specimens indicate that milling time of 30 hours is the minimum time required to reduce the particle sizes of the Mg-Ni mixed specimen from 3,5 ~10 μm into nanosize particles. It starts to agglomerate after 40 hours of milling due to the growth of magnetic properties of the powders and the change of crystal orientations into amorphous state.

FREE TERMS: High energy ball milling, Crystal structure

ABSTRAK

ANALISIS DIFRAKSI SINAR-X TERHADAP PEMADUAN MEKANIK PADA PEMBENTUKAN Mg2Ni. *Sintesa dan karakterisasi logam paduan Mg_2Ni yang dibuat dengan teknik pemaduan mekanik telah dilakukan. Bahan paduan di-*milling *dengan waktu* milling *bervariasi yakni 20, 25, 30, 35 dan 40 jam. Hasil pengukuran dengan menggunakan difraktometer sinar-X menunjukkan bahwa hasil pengolahan data atas hasil cacah difraktometer sinar-X sangat sesuai dengan hasil observasi. Hasil olahan menunjukkan bahwa spesimen terdiri dari tiga fasa, yaitu Mg_2Ni, MgO dan $MgNi_2$. Untuk waktu* milling *antara 20 dan 25 jam, fraksi massa fasa Mg_2Ni bertambah dari 42,19% menjadi 51,03%.* Milling *lanjutan hingga 40 jam akan mereduksi fraksi massa fasa Mg_2Ni menjadi 11,86%. Hal ini mungkin disebabkan adanya oksigen di dalam mesin* milling*, dan sebagai konsekuensinya akan menambah fraksi massa fasa $MgNi_2$. Disimpulkan bahwa waktu* milling *mempengaruhi pembentukan senyawa Mg_2Ni. Pada penelitian ini, waktu* milling *selama 25 jam adalah waktu terbaik untuk pembentukan fasa senyawa Mg_2Ni. Analisa mikrostruktur atas spesimen menunjukkan bahwa waktu* milling *30 jam adalah waktu minimum yang diperlukan untuk mereduksi ukuran partikel dari 3,5~10 μm menjadi partikel ukuran nano. Setelah* milling *selama 40 jam spesimen mulai*

menggumpal yang disebabkan oleh tumbuhnya sifat magnet serbuk dan terjadinya perubahan orientasi kristal menjadi amorf.

KATA KUNCI: High energy ball milling*, Struktur kristal*

I. INTRODUCTION

Hydrogen is the ideal means of storage, transport and conversion of energy for a comprehensive clean-energy concept. However, appropriate storage facilities, both for stationary and mobile applications, are complicated because of the very low boiling point of hydrogen (20.4 K at 1 atm) and its low density in the gaseous state (0.0071 g/cm^3). Furthermore, the storage of hydrogen in liquid or gaseous form imposes safety problems, in particular for mobile applications, e.g. the future zero-emission vehicle[1].

Metals can absorb hydrogen in atomic form and thereby act as hydrogen "sponges"[2]. Around 50 metallic elements of the periodic table can absorb hydrogen in great quantity and the possible choices of hydrogen storage materials are, therefore, enormous. Many scientific and engineering studies have been carried out of the hydriding-dehydriding in metals, especially in the development of such storage devices. Daimler-Benz, for example, in the early 1980s produced a car fueled by hydrogen where the storage tank was a chunk of FeTi metal alloy[3]. The volume of this storage devices is less than a factor of two greater than the equivalent gasoline tank, but the problem is that the hydride is 20 times heavier[4]. The only successful commercial large-scale application of metal hydrides storage so far is the metal hydride battery, which has supplied battery power to many small electrical appliances such as mobile phone and portable computers. Metal hydrides have so far not become useful as storage devices for hydrogen gas even though they have some distinct advantages over pressurized hydrogen gas, both improved safety and reduced volume.

Magnesium and its derived alloys are looked upon as promising candidates of hydrogen storage due to their high theoretical storage capacity (7.6 wt%), light weight and low cost. However, high operating temperatures and slow kinetics prevent them from practical application[5,6]. Multi component Mg base alloys have met with limited success in increasing kinetic dynamics and lowering the desorption temperature[7-8]. Efforts to seek new ternary Mg hydrides with favored reaction kinetics and temperature have not produced promising results[9-11]. A number of reports show that the reaction kinetics have been accelerated significantly, even at ambient temperature using nanostructures or amorphous Mg based materials synthesized by ball milling or mechanical alloying (MA)[12-14]. Unfortunately, the desorption temperature of the studied Mg based materials is still too high to be used practically. In most cases, it requires at least 250 °C to liberate hydrogen from magnesium hydrides. To explore the possibility and assess the reality of lower desorption temperatures, several amorphous/nanostructured composite Mg based materials have been investigated.

So far, the overwhelming majority of MA or mechanical ball milling (MM) processing has been carried out in either planetary (Fritsch) or mixer (SPEX) ball mills. The movement of balls in these mills is rather uncontrolled and chaotic. This may be one reason for some conflicting results on the hydriding /dehydriding properties of hydrogen storage nanocrystalline or amorphous powders reported by various research groups in the literature. On the other hand, there is a lack of systematic studies comparing hydriding properties of nanocrystalline powders fabricated by various ball milling techniques (i.e. types of mill).

ISSN 1907–2635
82/Akred-LIPI/P2MBI/5/2007

Recently, many hydrided materials have been found, especially for magnesium-based materials in the form of A_2B compounds, e.g. Mg_2Ni and Ti_2Ni. The promising hydrided material for the time being is Mg_2Ni. The Mg_2Ni compound is one of the hydrided materials developed to improve its weakness on hydriding/dehydriding properties of single Mg metal. Synthetic compound of Mg-Ni by using mechanical alloying is used in this method.

In this paper, we present recent results on the synthetic Mg-Ni compounds formation using SPEX type high energy ball milling.

II. EXPERIMENTAL

The milling experiments were performed in a SPEX 8000 type high energy ball milling (HEM). The materials used in this experiment were magnesium powder (Aremco, 99.8%, -270 mesh or about <3.5 μm) and nickel powder (Merck, 99.5%, <10 μm) with the atomic ratio of Mg:Ni = 2:1. The different initial powder particle sizes were blended together in a varied milling time. The operating procedure of the SPEX is as follows: the blending speed is set at 4500 rpm, running time 90 minutes and off time 30 minutes. This is called one cycle of milling. Figure 1 shows the SPEX 8000 used in the experiment.

(a) (b)

Figure 1. (a) High energy milling (HEM); (b) HEM vial

The HEM consists of a vial which is filled with balls moving spinally to comminute the powder of initial specimens into smaller sizes. The vials are made of stainless steel wih the diameter of 5.1 cm and 7.6 in length. The balls used are made of stainless steel with the diameter of the balls 12 mm. About 15 grams of Mg and Ni elements with atomic ratio of Mg:Ni = 2:1 is mixed together with balls and poured into the vial. The ball to specimens ratio is 8. The varied milling time is selected at 20, 25, 30, 35 dan 40 hours at room temperature.

Qualitative and quantitative analyses used in the experiment were conducted in a Philip, type PW1710, X-ray diffractometer using Cu as the anode tube and λ = 1.5406 Å. Continuous scanning was conducted at 0.02° step size and 0.5 second/step. To analyze the counting results, a RIETAN code developed by Fuji Izumi[15] was used. The observation and calculation results were compared according to the information obtained.

Microstructures of the specimens after millings were examined by using Scanning Electron Micrograph, JEOL type 840°.

III. RESULTS AND DISCUSSIONS

3.1. XRD Analysis

Figure 2 is the simulation results obtained using RIETAN code which represent the possibility of the Mg-Ni compounds formed due to the MA. The input data for calculation were copied from the International Crystalographic Table[16].

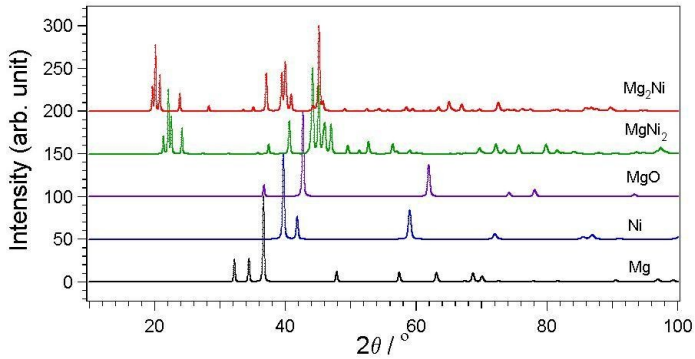

Figure 2. The Mg-Ni compounds simulated using the RIETAN code

The space group of Mg_2Ni crystal structure is P 62 2 2 (Vol. I, 180), hexagonal crystalline with lattice parameter of a = 5.204 62 Å, b = 5.204 62 Å, and c = 13.019 30 Å with the $\alpha = \beta = 90°$ and $\gamma = 120°$. The Wyckoff position or number of equivalent points per unit cell according to the Hirata's results[17] is presented in Table 1.

Table 1. Wyckoff position for Mg and Ni in the Mg_2Ni compound

Atom	Ocupation factor	x	y	z
Mg(1)	1.0	0.5000	0.0000	0.1103
Mg(2)	1.0	0.2864	0.3035	0.0000
Ni(1)	1.0	0.0000	0.0000	0.5000
Ni(2)	1.0	0.5000	0.0000	0.5000

The space group for MgO crystal structure is F m 3 m (Vol. I, 225), cubic crystalline with lattice parameters of $a = b = c$ = 4,22216 Å, and $\alpha = \beta = \gamma = 90°$. The Wyckoff position or number of equivalent points per unit cell according to the Kern's results[18] is presented in Table 2.

Table 2. Wyckoff position for Mg and O in the MgO compounds

Atom	Occupation factor	x	y	z
Mg	1.0	0.0000	0.0000	0.0000
O	1.0	0.5000	0.5000	0.5000

The space group of $MgNi_2$ crystal structure is P 63/m mc (Vol. I, 194), hexagonal crystalline with lattice parameter of a = 4.8600 Å, b = 4.8600 Å, and c = 15.7276 Å with $\alpha = \beta = 90°$ and $\gamma = 120°$. The Wyckoff position or number of equivalent points per unit cell according to the Stadelmaier's results[19] is presented in Table 3.

ISSN 1907–2635
82/Akred-LIPI/P2MBI/5/2007

Table 3. Wyckoff position for Mg and Ni in the $MgNi_2$ compounds

Atom	Occupation factor	x	y	z
Mg(1)	1.0	0.0000	0.0000	0.0959
Mg(2)	1.0	0.3330	0.6670	0.8401
Ni(1)	1.0	0.3330	0.6670	0.1329
Ni(2)	1.0	0.5000	0.0000	0.0000
Ni(3)	1.0	0.1666	0.3005	0.2500

The original XRD profiles after milling under the varied milling time are presented in Figure 3 and will be discussed in detail.

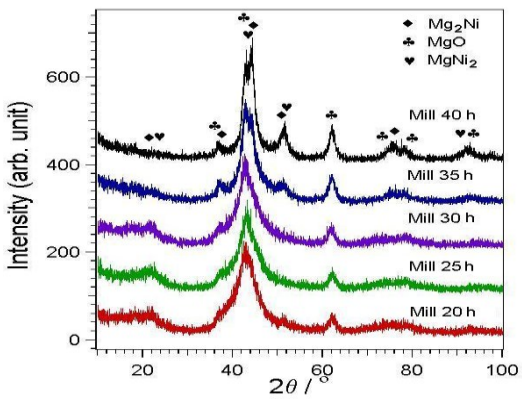

Figure 3. The XRD profiles on milling time of 20, 25, 30, 35 dan 40 hours

Figure 4 presents the XRD profiles under the varied milling time. According to the Hanawalt table, it is shown that the results obtained can be identified as the Mg_2Ni, MgO and $MgNi_2$ phases. Since the Hanawalt table cannot be used to identify the growth of each compounds, RIETAN code is used for quantitative measurement.

Analyses of the XRD profile using Rietveld iteration method by inserting the crystal structures parameters of the above three phases into the calculation exhibited that after 20 iterations the *g* factor (occupation factor) for Mg and Ni is greater than 1.0. Continuous refinement was conducted by assuming the *g* factor for Mg and Ni, $g_{Mg,Ni}$ = 1.0 and the calculation results exhibited that all lattice parameters are normal. It should be noted that there is no refinement for the light weight atom such as oxygen. By using the IGOR Pro software, the calculation and observation curves can be reconstructed and presented in the following figures. Figure 4 shows the fitting curve for the Mg_2Ni specimen after 20 hours of milling. The symbol (+) represents the observation, the symbol (–) represents the calculation, Miller index is represented by (|) and the difference between observation and calculation is represented by symbol (-). The difference between the two curves indicates the quality of fitting method, i.e the more straight of the line the quality of fitting is good and in accordance to the standard

reference of the specimen[19]. Figure 4 shows that the XRD peak profiles for Mg_2Ni, MgO and $MgNi_2$ are close together while the lattice parameters, R factor (criteria of fit) and S (goodness of fit) are presented in Table 4.

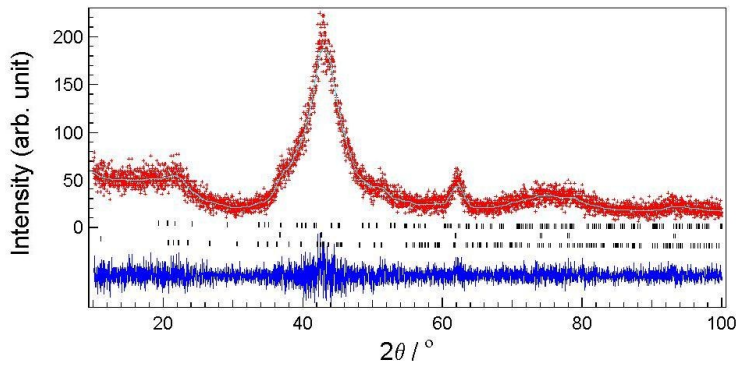

Figure 4. Refinement result of the XRD profile for the Mg_2Ni compound after 20 hours of milling

By using the same method, the XRD profiles for observation and calculation for 25, 30, 35 and 40 hours of milling are presented in Figures 5 – 8 and and Tables 5 – 8.

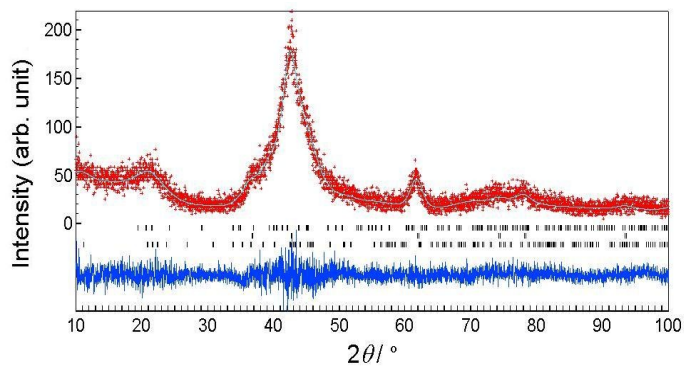

Figure 5. Refinement result of the XRD profile for the Mg_2Ni compound after 25 hours of milling

ISSN 1907–2635
82/Akred-LIPI/P2MBI/5/2007

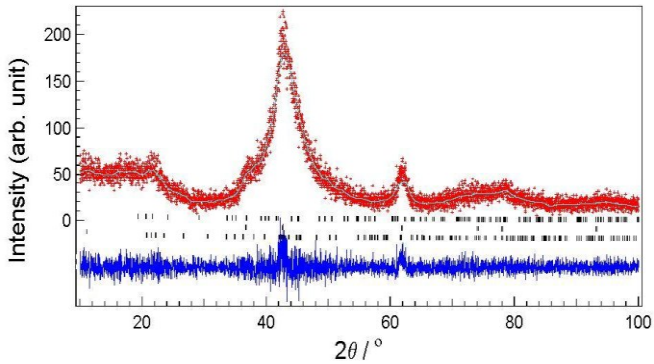

Figure 6. Refinement result of the XRD profile for the Mg_2Ni compound after 30 hours of milling

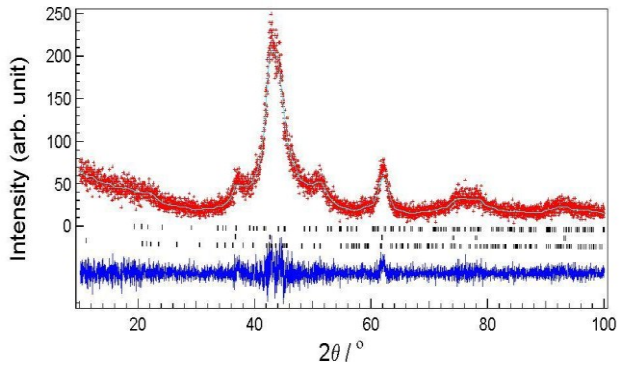

Figure 7. Refinement result of the XRD profile for the Mg_2Ni compound after 35 hours of milling

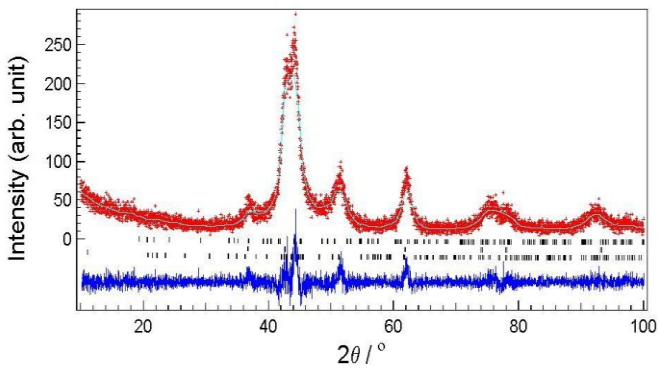

Figure 8. Refinement result of the XRD profile for the Mg_2Ni compound after 40 hours of milling

Table 4. The lattice parameter, position of atom, criteria of fit and goodness of fit for the Mg_2Ni specimen after 20 hours of milling

Phase and lattice parameter (Å)	Atom	*g*	Atom fraction coordinate			R factor (%)
			x	y	z	
Mg_2Ni a = b = 5.320(8) c = 12.323(3)	Mg(1)	1.0	0.5	0	0.111(1)	R_{wp} = 20.07
	Mg(2)	0.98(9)	0.288(4)	0.297(2)	0	R_I = 7.46
	Ni(1)	1.0	0	0	0.5	R_F = 4.14
	Ni(2)	0.98(2)	0.5	0	0.5	S = 1.29
MgO a = b = c = 4.246(3)	Mg	0.99(2)	0	0	0	R_I = 7.88
	O	1.0	0.5	0.5	0.5	R_F = 4.15
$MgNi_2$ a = b = 4.963(7) c = 16.045(3)	Mg(1)	1.0	0	0	0.095(4)	R_I = 7.15
	Mg(2)	1.0	0.3330	0.6670	0.846(4)	R_F = 4.01
	Ni(1)	1.0	0.3330	0.6670	0.124(3)	
	Ni(2)	1.0	0.5	0	0	
	Ni(3)	0.99(1)	0.126(1)	0.311(4)	0.25	

Table 5. The lattice parameter, position of atom, criteria of fit and goodness of fit for the Mg_2Ni specimen after 25 hours of milling

Phase and lattice parameter (Å)	Atom	*g*	Atom fraction coordinate			R factor (%)
			x	y	z	
Mg_2Ni a = b = 5.299(1) c = 12.425(1)	Mg(1)	1.0	0.5	0	0.116(4)	R_{wp} = 17.34
	Mg(2)	0.96(7)	0.307(2)	0.267(1)	0	R_I = 5.08
	Ni(1)	1.0	0	0	0.5	R_F = 3.34
	Ni(2)	0.88(4)	0.5	0	0.5	S = 1.06
MgO a = b = c = 4.237(1)	Mg	0.97(2)	0	0	0	R_I = 4.61
	O	1.0	0.5	0.5	0.5	R_F = 2.99
$MgNi_2$ a = b = 4.919(1) c = 15.912(2)	Mg(1)	1.0	0	0	0.094(1)	R_I = 4.64
	Mg(2)	1.0	0.3330	0.6670	0.848(1)	R_F = 3.18
	Ni(1)	1.0	0.3330	0.6670	0.132(4)	
	Ni(2)	1.0	0.5	0	0	
	Ni(3)	0.98(5)	0.199(1)	0.323(1)	0.25	

Table 6. The lattice parameter, position of atom, criteria of fit and goodness of fit for the Mg_2Ni specimen after 30 hours of milling

Phase and lattice parameter (Å)	Atom	*g*	Atom fraction coordinate			R factor (%)
			x	y	z	
Mg_2Ni a = b = 5.311(8) c = 12.096(3)	Mg(1)	1.0	0.5	0	0.112(2)	R_{wp} = 20.69
	Mg(2)	0.99(6)	0.285(2)	0.302(3)	0	R_I = 8.65
	Ni(1)	1.0	0	0	0.5	R_F = 4.78
	Ni(2)	0.98(4)	0.5	0	0.5	S = 1.29
MgO a = b = c = 4.252(3)	Mg	0.99(2)	0	0	0	R_I = 9.44
	O	1.0	0.5	0.5	0.5	R_F = 4.90
$MgNi_2$ a = b = 4.937(5) c = 15.903(2)	Mg(1)	1.0	0	0	0.094(4)	R_I = 8.26
	Mg(2)	1.0	0.333	0.667	0.845(4)	R_F = 4.59
	Ni(1)	1.0	0.333	0.667	0.127(3)	
	Ni(2)	1.0	0.5	0	0	
	Ni(3)	0.99(1)	0.124(1)	0.309(4)	0.25	

ISSN 1907–2635
82/Akred-LIPI/P2MBI/5/2007

Table 7. The lattice parameter, position of atom, criteria of fit and goodness of fit for the Mg_2Ni specimen after 35 hours of milling

Phase and lattice parameter (Å)	Atom	*g*	Atom fraction coordinate			R factor (%)
			x	y	z	
Mg_2Ni a = b = 5.373(9) c = 11.551(3)	Mg(1)	1.0	0.5	0	0.110(3)	R_{wp} = 23.79
	Mg(2)	0.99(9)	0.286(3)	0.303(5)	0	R_I = 10.50
	Ni(1)	1.0	0	0	0.5	R_F = 5.78
	Ni(2)	0.98(1)	0.5	0	0.5	S = 1.26
MgO a = b = c = 4.253(2)	Mg	0.99(1)	0	0	0	R_I = 14.14
	O	1.0	0.5	0.5	0.5	R_F = 6.80
$MgNi_2$ a = b = 4.952(4) c = 16.033(2)	Mg(1)	1.0	0	0	0.095(4)	R_I = 11.17
	Mg(2)	1.0	0.333	0.667	0.847(6)	R_F = 5.82
	Ni(1)	1.0	0.333	0.667	0.128(3)	
	Ni(2)	1.0	0.5	0	0	
	Ni(3)	0.99(2)	0.148(8)	0.311(4)	0.25	

Table 8. The lattice parameter, position of atom, criteria of fit and goodness of fit for the Mg_2Ni specimen after 40 hours of milling

Phase and lattice parameter (Å)	Atom	*g*	Atom fraction coordinate			R factor (%)
			x	y	z	
Mg_2Ni a = b = 5.308(4) c = 11.121(3)	Mg(1)	1.0	0.5	0	0.110(2)	R_{wp} = 33.14
	Mg(2)	1.0	0.286(4)	0.303(5)	0	R_I = 22.12
	Ni(1)	1.0	0	0	0.5	R_F = 12.36
	Ni(2)	1.0	0.5	0	0.5	S = 1.30
MgO a = b = c = 4.253(8)	Mg	1.0	0	0	0	R_I = 27.56
	O	1.0	0.5	0.5	0.5	R_F = 14.25
$MgNi_2$ a = b = 4.957(2) c = 16.053(1)	Mg(1)	1.0	0	0	0.095(8)	R_I = 19.36
	Mg(2)	1.0	0.333	0.667	0.840(1)	R_F = 11.64
	Ni(1)	1.0	0.333	0.667	0.132(9)	
	Ni(2)	1.0	0.5	0	0	
	Ni(3)	1.0	0.166(5)	0.300(5)	0.25	

Figures 4, 5, 6, 7 and 8 show that all profiles are in good agreement between the observation and the calculations. This can be seen from the small number of *R* and *S* factors. It can be concluded that all of the refinement works are well fitted to the original data for Mg-Ni compounds under the varied milling times.

Around the 20° regions, the specimen after 20 hours of milling exhibits peaks belonging to Mg_2Ni (19.33°) and $MgNi_2$ (21.58°). The peaks formed were broadened which may be due to the particle sizes contributions. This can be proven from data of the 25 hours of milling where the peaks were becoming sharp. At 30 hours of milling, the peaks on the 20° disappear, which indicates that the number of mass fractions of Mg_2Ni dan $MgNi_2$ phases decrease stepwisely.

Similarly, observation on the regions of 37°, 44° and 52° indicate that the strong peaks can be seen in the regions of 39.23°, 40.38°, 45.13°, 50.29° and 52.73° that be explained as follows. At 20 hours of milling the Mg_2Ni compound grows fairly and becomes strong after 25

hours of milling. Unlike Mg_2Ni, the $MgNi_2$ peaks in the regions 36.50°, 40.01°, 42.75°, 43.21° and 50.60° decrease and only at the angle of 51.58° the peak grows a little. Nevertheless, the peaks indicated that MgO phase grows fairly on increased milling times. Figure 9 presents the calculation results after refinement.

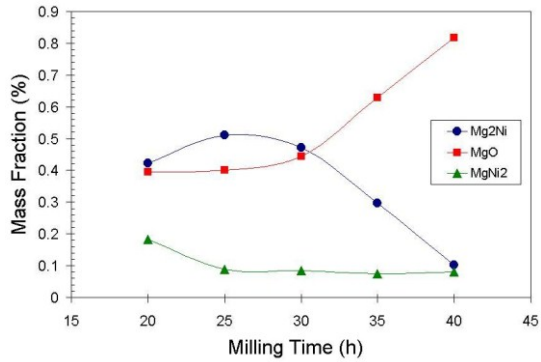

Figure 9. Milling time versus mass fraction of Mg_2Ni, MgO and $MgNi_2$ formation

The increase of the mass fraction of MgO is suggested due to the presence of oxygen during milling. Referring to Figure 8 and assuming that the amount of oxygen can be eliminated, the formation of Mg_2Ni can be increased significantly and the formation of $MgNi_2$ compound can be suppressed.

3.2. Microstructure Analysis

Figures 10, 11, 12, 13 and 14 show the microstructures of Mg-Ni powders after 20, 25, 30, 35 and 40 hours of milling. During milling for 20 hours the number of reducing particle into the smaller one seems to be very slow and after milling for 30-35 hours the number of nanosize particles can be observed very clearly to be <100 nm. In addition to the milling times, after milling of 40 hours the particles start to agglomerate which is due to the growing of the magnetic properties of the particles and the change of crystal orientations into amorphous state, though the number of the nanosize particles increase significantly. From the microstructures point of view combined with the XRD results, it is observed that the formation of Mg_2Ni and $MgNi_2$ compounds have taken place during 20 hours of milling. The presence of oxygen in the machine results in the formation of MgO.

During milling, the longer the milling time is the stronger the formation of Mg_2Ni and $MgNi_2$ becomes. It can be shown that after 40 hours of milling the peaks of the two compounds increase sharper and start splitting and the crystallite nano-size has been completed. In addition, the particle size of MgO also becomes smaller, which can be seen from its broadening peaks. The broadening peaks of MgO affects the peaks of Mg_2Ni and $MgNi_2$ (the peak at 40° consists of the three compounds).

From the microstructure observation, it is concluded that at milling time of 30 hours all powders converted into Mg_2Ni compound and nanosize particles.

ISSN 1907–2635
82/Akred-LIPI/P2MBI/5/2007

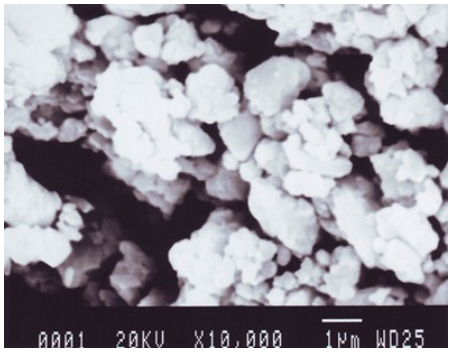

Figure 10. Nanosize of Mg-Ni powders after 20 hours of milling

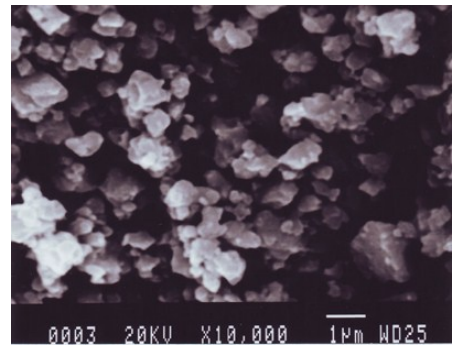

Figure 11. Nanosize of Mg-Ni powders after 25 hours of milling

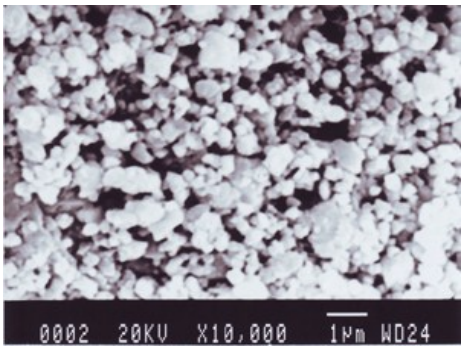

Figure 12. Nanosize of Mg-Ni powders after 30 hours of milling

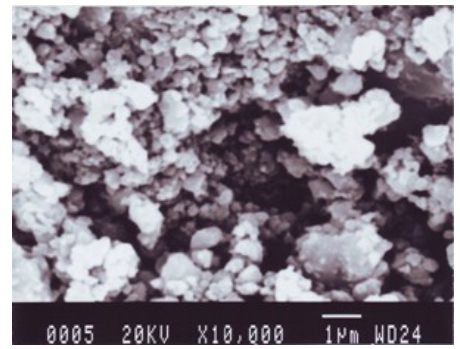

Figure 13. Nanosize of Mg-Ni powders after 35 hours of milling

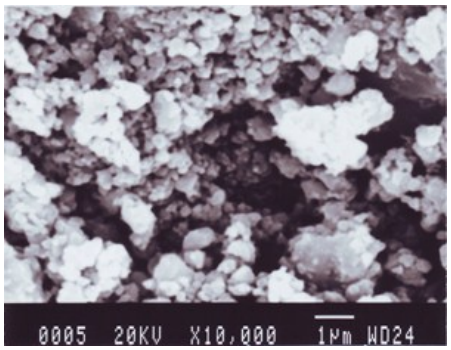

Figure 14. Nanosize of Mg-Ni powders after 40 hours of milling

IV. CONCLUSION

Synthesis of the Mg_2Ni compound has been examined using mechanical alloying technique. The XRD analysis exhibited that the observation and the calculation results indicate the formation of Mg_2Ni, MgO and $MgNi_2$ compounds after 20 to 40 hours of milling. The mass fraction of Mg_2Ni compounds increases up to 51.03% for milling time of 25 hours and then reduces to 11.86% on continuous milling due to the presence of oxygen.

The nanosize particles can be formed after 30 hours of milling and start to agglomerate after 40 hours of milling due to the growth of magnetic properties of the powders and the change of crystal orientations into amorphous state.

Continuous experiment in the form of hydriding–dehydriding properties of the Mg_2Ni powder obtained by the current method will be conducted in the near future in order to investigate the hydrogen capacity of the specimen.

V. ACKNOWLEDGEMENT

The author would like to acknowledge the Ministry of Research and Technology for providing the financial support for this program. Great thanks are also addressed to all workers in the Center for Nuclear Fuel Technology and the Center for Nuclear Industry Materials at National Nuclear Energy Agency for their accommodation.

VI. REFRENCES

1. DORNHEIM, M., KLASSEN, T., and BORMANN, R., “Hydrogen Storage Materials”, Institute for Materials Research, GKSS Research Center, Geesthacht, Germany. (Internet)
2. ARNASON, B., and SIGFUSSON, T.I., Int. J. Hydrogen Energy, Vol.25, 2000, p.389.
3. BUCHENER, H., and POVEL, R., Int. J. Hydrogen Energy, Vol.7, 1982, p.259.
4. FUKAI, Y., “The Metal-Hydrogen System – Basic Bulk Properties”, Verlag, Berlin, 1993.
5. REILLY, J.J., and WISWALL, R.H., Inorg. Chem., Vol. 6, 1967, p.2220.
6. DARRIET, B., et al., Int. J. Hydrogen Energy, N2, 1980, p.173.
7. KARTY, A., GRUNZWIG-GENOSSAR, J., and SUDMAN, P.S., J. Appl. Phys., V50, N11, 1979, p.7200.
8. DOUGLASS, D.L., Met. Trans., 6A, 1975, p.2186.
9. AU, M., WU, J., and WANG, Q.D., Int. J. Hydrogen Energy, V20, N2, 1995, p.141.
10. AEBISCHER, H.A., and SCHALPBACH, L., Z. Phys. Chem., 179.S, 1993, p.21.
11. KADIR, K., and NOREUS, D., Z. Phys. Chem., 179.S, 1993, p.243.
12. HUANG, B., YVON, K., and FISHER, P., J. Alloys Comp., Vol.227, 1995, p.121.
13. ZALUSKA, A., ZALUSKI, L., and SROM-OLSEN, J.O., J. Alloys Comp., Vol.228, 1999, p.217.
14. LIANG, G., HUOT, J., BOILY, S., NESTE, A.V., and SCHULTZ, R., J. Alloys Comp., Vol. 348, 2003, p.319.
15. IZUMI, F., “RIETAN Manual”, 1994. (Private communication).
16. NORMAN, F., HENRY, M., and KATLEEN, L., Editors, International Tables for X-Ray Crystallography, Vol. 1, Symmetry Groups, the Kynoch Press, England, 1969.
17. SOUBEYROUX, J.L., et al., Mater. Res. Bull., Vol.19, 1984, p.895.
18. SCHMAHL, N.G., BARTHEL, J., and EIKERLING, G.F., Z. Anorg Allg. Chem., Vol.332, 1964, p.230.
19. STADELMEIR, et al., North Carolina State Univ., Releigh, N.C, USA. (Private communication)